# Fractal structures in a generalized square map with exponential terms*

Li Xian-Feng(李险峰)[a)†], Chu Yan-Dong(褚衍东)[a)], and Zhang Hui(张 惠)[a)b)]

[a)] School of Mathematics, Physics and Software Engineering, Lanzhou Jiaotong University, Lanzhou 730070, China
[b)] School of Mechanical Engineering, Lanzhou Jiaotong University, Lanzhou 730070, China

(Received 10 August 2011; revised manuscript received 18 September 2011)

Fractal structures in a generalized squared map with exponential terms are expanded in this paper. We describe how complex behaviors can arise as the parameters change. The appearances of different kinds of fractal structures, in both the attractive and the divergent regions, and most interestingly, on small regular islands embedded in the chaotic region, are manifested to have a variety of extraordinary geometries in the parameter plane.

**Keywords:** discrete map, exponential term, parameter plane, Lyapunov fractal

**PACS:** 02.30.Rz, 05.45.Pq, 05.45.Ac **DOI:** 10.1088/1674-1056/21/3/030203

## 1. Introduction

It is well known that chaotic discrete maps consisting of difference equations commonly arise from nonlinear dynamical systems investigated in many fields of science and society,[1−9] which also can be aided to reduce the dimensions of ordinary differential equations (ODEs) by utilizing the surface of section technique of the Poincaré map.[10−13] Inherently, in the theory of dynamical systems, the exponential map can be used as the evolution function of a discrete nonlinear dynamical system.[14,15] It is notable here that the study of discrete dynamical systems has been primarily limited to maps of an interval of diffeomorphisms.[16] The diffeomorphisms of a plane exhibit some of the familiar properties of the two-dimensional (2D) Hénon map.[2] In this paper, we introduce a new 2D generalized squared map with exponential terms, which couples with two one-dimensional (1D) endomorphisms of squared maps with exponential terms.[17] The governing equations describing the map can be rewritten as

$$\begin{cases} x_{n+1} = b(\,\mathrm{e}^{-cx_n^2} - x_n^2) + ay_n, \\ y_{n+1} = b(\,\mathrm{e}^{-cy_n^2} - y_n^2) + ax_n, \end{cases} \tag{1}$$

where $x$ and $y$ are the real variables, $a$, $b$, and $c$ are the real parameters. Bao *et al.*[17] created lots of beautiful attractors possessing chaotic (or non-chaotic) and symmetric properties within a wide range of parameter values. Some ubiquitous nonlinear dynamics were illustrated, such as periodic windows, symmetric distributions of Lyapunov diagrams, and different types of bifurcation. Here, our aim is to study the fractal structures of map (1). The dynamics involve various transitions characterized principally by codimension-2 bifurcations, fractal basins, and Lyapunov fractals. Due to the theoretical and the practical difficulties in the study, numerical technologies will presumably play a role in such efforts.

## 2. Fractal bifurcation structure

### 2.1. Symmetry coupling

As a matter of fact, each equation of map (1) can be viewed as a 1D endomorphism imbedded into itself mutually, that is, into a 2D diffeomorphism. This fact demonstrates that attractors $\{x_n, y_n\}$ of map (1) are symmetric about the $x$–$y$ axis. The diffeomorphisms can be considered as a model that only gives rise to a set of bifurcations in the nature of fractal characteristics. We study the diffeomorphisms depending on two parameters, namely, $a$ and $b$. Parameter $c$ can be adjusted to some relatively large numbers to accelerate the exponential convergence. Here $\{x_n, y_n\}$ is the sequence of iterations converging to a bounded region of rationality as the iterate time $n \to \infty$. In this paper,

*Project supported by the National Natural Science Foundation of China (Grant No. 11161027) and the Natural Science Foundation of Gansu Province, China (Grant No. 1010RJZA067).

†Corresponding author. E-mail: lixf1979@vip.qq.com

© 2012 Chinese Physical Society and IOP Publishing Ltd

isoclines are calculated simply in the $a$–$b$ parameter plane to reveal the existence of the Neimark–Sacker bifurcation (NSB), denoted as the quasi-periodicity. Outside these parameter regimes, the ever-changing parameters will give rise to bifurcations, thereby complicate the dynamics, which often involve chaos, hyperchaos, or even diverge to infinity.

The fixed point $\{x_n^*, y_n^*\}$ of map (1) satisfies

$$\begin{cases} x_n = b(\mathrm{e}^{-cx_n^2} - x_n^2) + ay_n, \\ y_n = b(\mathrm{e}^{-cy_n^2} - y_n^2) + ax_n. \end{cases} \tag{2}$$

Unfortunately, the set of difference equations (2) has no accurate analytical solution, which means that we have to turn to numerical root-finding algorithms. The Newton–Raphson method is one of the classical numerical root-finding methods and is often employed to find the asymptotical approximate solutions or to locate the initial conditions if there are two or more distinct roots. Figure 1 shows the locations of the set of stable fixed points in the $a$–$b$ plane. After numerous computer calculations, the result shows that the stable fixed points only exist in the collision boundary between escape and period-1 ($P_1$) regimes.

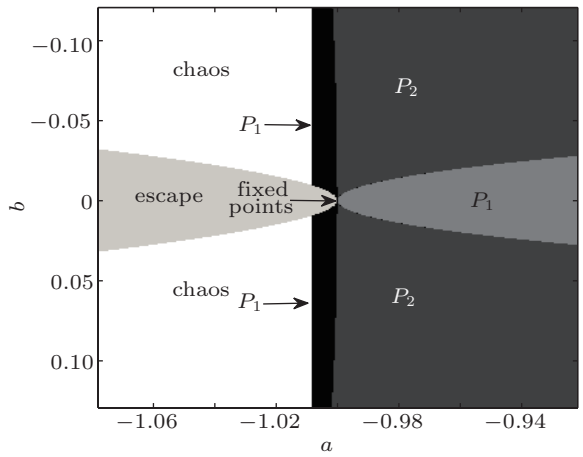



**Fig. 1.** Locations of the set of stable fixed points in the $a$–$b$ plane.

## 2.2. Searching for NSB points

Once the location and the stability of one fixed point are confirmed, the instability conditions can be derived from the eigenvalues of the Jacobian matrix of map (1). Local bifurcations occur when the modules of the eigenvalues lie on the unit circle. The type of bifurcation derived from a closed invariant curve from a fixed point is called the NSB in 2- or higher-dimensional iteration map.[16,18–21] To be more exact, in a 2D map, the critical condition for an NSB requires that at the critical threshold of the bifurcation parameters, a pair of complex conjugate eigenvalues lie on the unit circle.

Suppose that $\boldsymbol{T}$ is a discrete map, $\boldsymbol{T}: \mathrm{R}^n \to \mathrm{R}^n$; $\boldsymbol{\chi} \to \boldsymbol{T}(\boldsymbol{\chi})$, $\boldsymbol{\chi} \in \mathrm{R}^n$; $\lambda_1$ and $\lambda_2$ are two real control parameters; $\boldsymbol{T}$ is $\mathbb{C}^\infty$ for $\lambda_1$, $\lambda_2$, and $\boldsymbol{\chi}$. The $\boldsymbol{\chi}_0$ is a fixed point if $\boldsymbol{T}(\boldsymbol{\chi}_0) = \boldsymbol{\chi}_0$. At $\boldsymbol{\chi}_0$, a pair of complex conjugate multipliers are $\rho$ and $\bar{\rho} = r\,\mathrm{e}^{\pm \mathrm{i}\,\theta} = r(\cos(\theta) \pm \mathrm{i}\sin(\theta))$, where $r$ is the radius, and $\theta$ is the argument. In the meantime, $r$ and $\theta$ determine the stability and the angular velocity of the local linear space about $\boldsymbol{\chi}_0$. The $\boldsymbol{J}$ denotes the Jacobian matrix of map $\boldsymbol{T}$ at $\boldsymbol{\chi}_0$. The characteristic equation is $\hbar = \det[\boldsymbol{J} - r\,\mathrm{e}^{\pm \mathrm{i}\,\theta}] = \Re\hbar + \mathrm{i}\,\Im\hbar = 0$. If $\boldsymbol{\chi}_0$ is the fixed point, the condition of the fixed point with argument $\theta$ is

$$\boldsymbol{F} = \begin{bmatrix} \boldsymbol{T}(\boldsymbol{\chi}_0) - \boldsymbol{\chi}_0 \\ \Re\hbar \\ \Im\hbar \end{bmatrix} = \boldsymbol{0}. \tag{3}$$

Then the Jacobian matrix for Newton's method is

$$\boldsymbol{J}_{\boldsymbol{F}} = \begin{bmatrix} \dfrac{\partial \boldsymbol{T}}{\partial \boldsymbol{\chi}_0} - \boldsymbol{I}_n & \dfrac{\partial \boldsymbol{T}}{\partial \lambda_1} & \dfrac{\partial \boldsymbol{T}}{\partial r} \\ \dfrac{\partial \Re\hbar}{\partial \boldsymbol{\chi}_0} & \dfrac{\partial \Re\hbar}{\partial \lambda_1} & \dfrac{\partial \Re\hbar}{\partial r} \\ \dfrac{\partial \Im\hbar}{\partial \boldsymbol{\chi}_0} & \dfrac{\partial \Im\hbar}{\partial \lambda_1} & \dfrac{\partial \Im\hbar}{\partial r} \end{bmatrix}. \tag{4}$$

For a fixed $\theta \in [0, \pi]$, $(\boldsymbol{\chi}_0, \lambda_1, r) \in \mathrm{R}^{n+2}$ forms an isocline in the parameter plane $\lambda_1$–$\lambda_2$.[20] When $0 \le r < 1$, the fixed point is stable, while $1 < r < \infty$, the fixed point is unstable. The NSB takes place at $r = 1$. According to the aforesaid theory and methods, the NSB curves are obtained with the aid of a computer by point-to-point searching in the parameter plane. As shown in Fig. 2, due to the exponential terms, two symmetric NSB curves are not simple line segments as shown by the other generalized planar maps.[18–21]

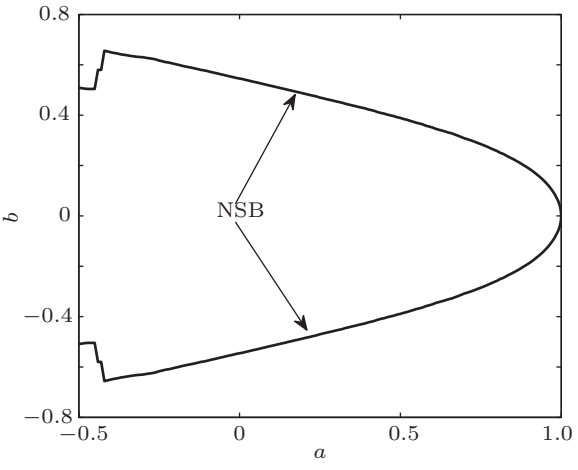



**Fig. 2.** Symmetric NSB curves in the $a$–$b$ plane of map (1).

## 2.3. Parameter space

Bifurcation phenomena involving the variation of just one single parameter, referred to as codimension-1 bifurcations, are now reasonably well understood. In contrast, fragmentary information is available about much more realistic situations that require the simultaneous variation of at least two independent parameters, referred to as codimension-2 bifurcations, which are necessary for studying the structures of phase diagrams in the parameter planes of chaotic systems, such as periodic and aperiodic motions, islands embedded in the chaotic region, periodic or chaotic hubs, and infinite-hierarchy nested spirals.[22] Those novel regularities are not properties of isolated solutions but can be recognized by contemplating large families of solution in an ordered way. In principle, this is an appropriate and efficient way to obtain the collective information about those entire complex motions in the parameter space.[23] One of our propositions here is to describe the regular self-organization observed using as much computer-time as possible to ensure that almost all orbits converge into their corresponding attractors, and to generate higher resolution images to discriminate and classify periodic and aperiodic asymptotic steady states over extended parameter regions of interest. Figure 3 displays different lower periodic motions with distinct colors, where $a$ and $b$ are in an elaborate rectangular grid of $[-1.5, 1] \times [-2, 2]$. The resolution of the image is $5001 \times 5001$. And we can better visualize that two period-doubling bifurcation (PDB) cascades stretch alternatively along two sides of the line $b = 0$. However, we need to state that the chaotic regions are intended to be

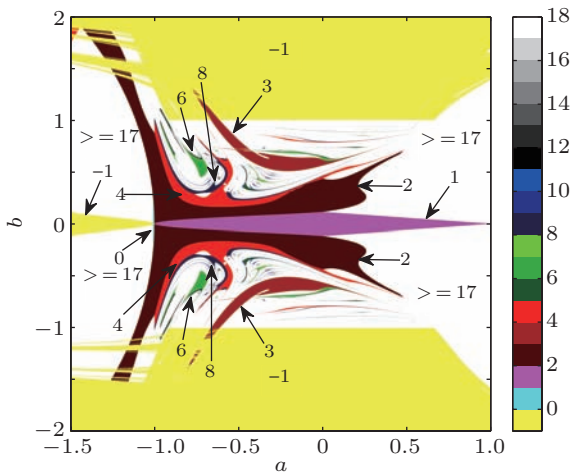



**Fig. 3.** (colour online) Generic structure of parameter space.

allocated as the domains with periods greater than or equal to 17 for the close observation of the distribution domains of other relatively low periods from 0 to 16. The domains, in which the solutions of map (1) diverge to $\infty$, are indicated by $-1$.

Considering the symmetry property of parameter $b$ and to meticulously observe the inner structures of the chaotic region, we magnify the part of interest with an identical resolution in Fig. 4.

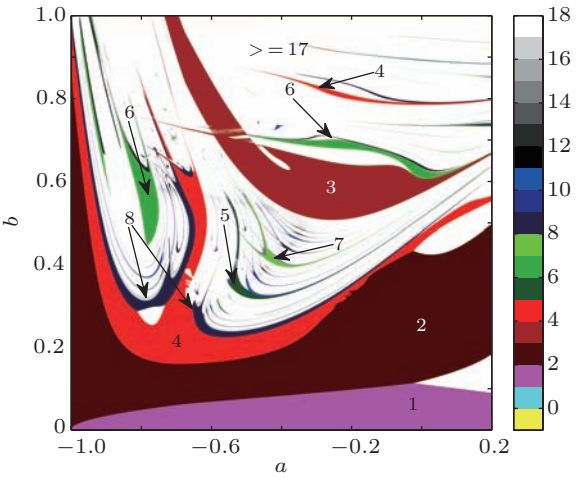



**Fig. 4.** (colour online) Magnified parameter region of interest.

There are two intriguing fragments considered, because there are so many small regular islands scattering in the chaotic region. One has innumerable infinite period-adding[24] (PA) islands embedded in the white background denoting chaos. At first sight, each of these shrimp-like islands has a self-similar shape, or loosely say, an approximately or stochastically self-similar shape. The self-similarity is the trait that makes the fractals what they are, zooming in on the image reveals smaller and smaller parts that resemble the whole. Therefore, each island can be regarded as locally-connected cycle spores on the Mandelbrot set, and has a fractal structure.[25] It can be found in many nonlinear systems, including discrete-time,[26] continuous-time,[27] and nonsmooth dynamical systems.[28] Figure 5 shows the scenarios of PA cascades. The colors indicate the relatively high periods characterizing the different islands from 0 to 64, each of them also has its own isolated infinite period-doubling (PD) cascade. Expressly, the main body of the largest shrimp is a $P_{12}$ region. When reducing $a$ and increasing $b$, the adding cascade of the main islands is recognized as

$$12 \to 16 \to 20 \to 24 \to 28 \to 32 \to 36 \cdots \infty \to 4.$$

Notice that with the exception of the first few periods of the cascade, all remaining periods emerge perfectly aligned along a specific direction in the parameter space. For the above cascade, the direction is well

approximated by a straight line

$$b = -4.7297a - 2.3090.$$

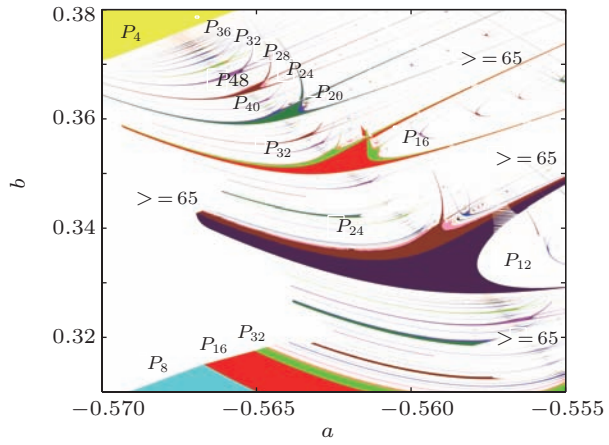



**Fig. 5.** (colour online) PA and PD cascades in the magnified parameter plane.

Another phenomenon we noticed is that the second largest islands, which are coterminous with the main islands, also have similar adding cascades to that of the main islands when we reduce $a$ and increase $b$

$$24 \to 32 \to 40 \to 48 \cdots \infty \to 4.$$

In the meantime, an obvious PD cascade can also be observed, which is marked as

$$P_8 \to P_{16} \to P_{32} \cdots \to \infty.$$

Another region is worth paying close attention to. As shown in Fig. 6, there are two conjoint $P_{18}$ windows embedded in the chaos region, and each of them has

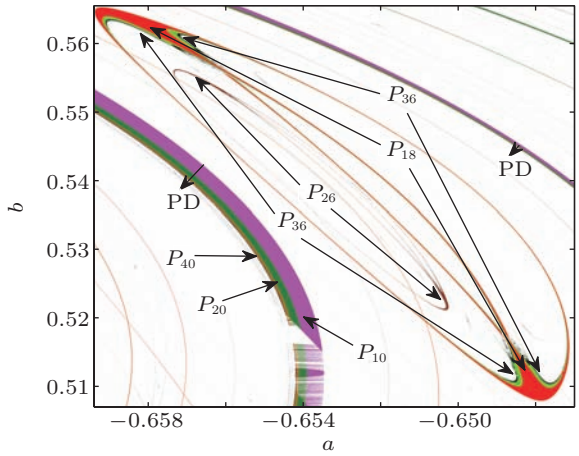



**Fig. 6.** (colour online) Conjoint PD windows.

a relatively independent PD cascade. This does not mean unattached and overlapping. We still can find more than a pair of conjoint periodic windows, two conjoint $P_{36}$, two conjoint $P_{72}, \cdots$, until chaos occurs. Nonetheless, another homologous behavior reappears beginning with two conjoint $P_{26}$, and goes on. The phenomenon explains the existence and the interlacing structure of chaotic and periodic hubs. In addition, a relatively wide PD window and a narrow PD window, whichboth have the same initiating period, $P_{10}$, are also labelled.

## 3. Fractal basins

As is now well known, an attractor of a dynamical system is a subset of the state space, to which the orbits originating from the typical initial conditions converge as time increases. Notwithstanding deterministic dynamical systems have coexisting attractors, whose appearances are determined by the initial conditions. The coexisting attractors can correspond to periodic, quasi-periodic, or aperiodic behaviors of different types.[29] For such an attractor, its basin of attraction is a set of initial conditions leading to long-time behavior that approaches that attractor. Thus the qualitative behavior of the long-time motion of a given system can be fundamentally different depending on which basin of attraction the initial condition lies in. With the corresponding initial conditions, map (1) can undergo different bifurcation cascades to chaos, mainly PDB and NSB in Ref. [17]. Recall that map (1) has a significant symmetry of variables $x$ and $y$. If the initial condition is chosen as $x_0 = y_0$, to some extent, map (1) can be reduced into a 1D discrete system

$$x_{n+1} = b(\mathrm{e}^{-cx_n^2} - x_n^2) + ay_n. \tag{5}$$

Thus the NSB cannot take place in map (5). From this viewpoint, $x_0 \neq y_0$ is the necessary condition for basins of attraction of quasi-periodic attractors. In striking contrast, the trajectories of one nonlinear system can always diverge to infinity for sets of initial conditions, named the exit basins. The exit basin of a particular exit is the set of initial conditions that yields escape through such an exit. As expected, these exit basins, or escape basins, as well as the basins of bounded attractors, exhibit fractal boundaries and the Wada property.[30] As shown in Figs. 7(a)–7(d), the basins of the bounded chaotic attractors suffer erosion effects as the control parameter $b$ decreases.

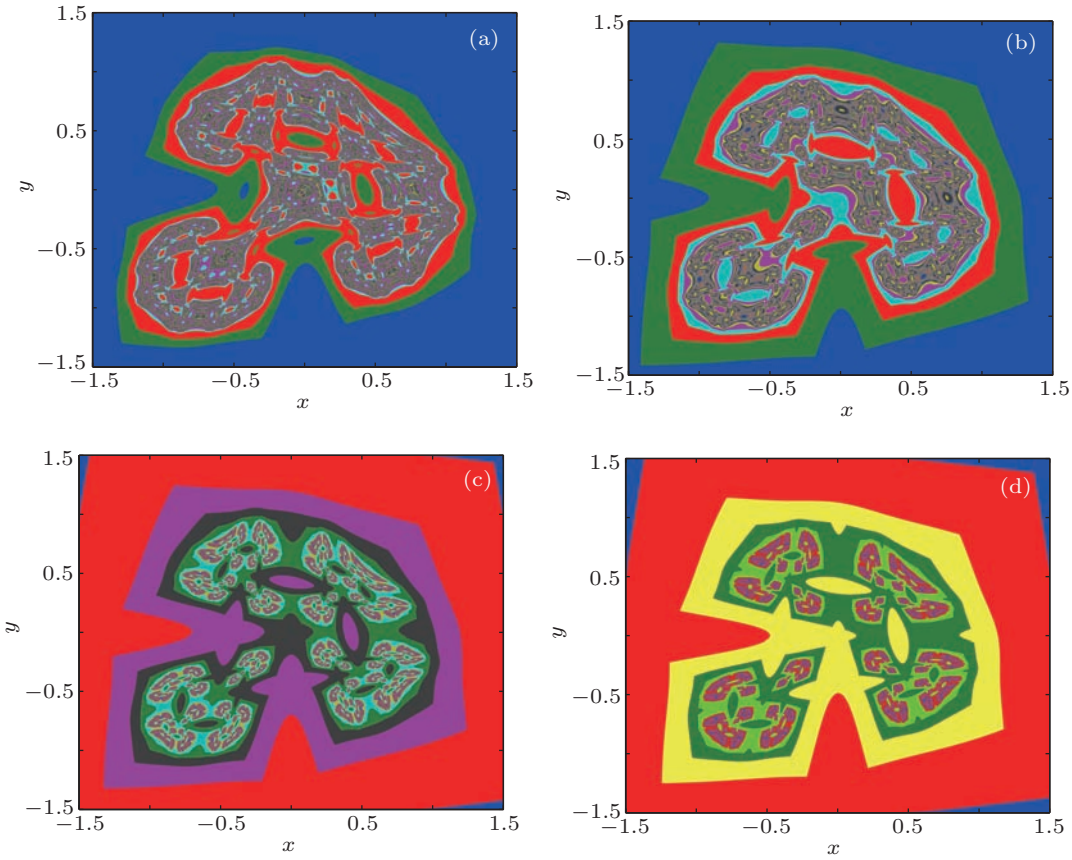



**Fig. 7.** (colour online) Erosion effects of basins of bounded chaotic attractors. Control parameter $b$ in panels (a)–(d) are –1, –1.1, –1.2, and –1.3, respectively.

## 4. Lyapunov fractals

Lyapunov fractals are fascinating bifurcational fractals derived from a simple extension of the 1D logistic map by Markus.[31] The Lyapunov fractal, particularly in a multi-parameter control system, is interlaced by the maximal Lyapunov exponents to discriminate the regions of stability and chaotic motions in a selected phase space. Besides their unexpected beauty, ground-breaking visual effect, and forceful artistic quality, the Lyapunov fractals can also supply more important information about the dynamics of a nonlinear system with many intermingled sequences of the parameter values. First of all, using the sign of the largest Lyapunov exponent, the regions of stability and chaotic behavior can be discriminated. Furthermore, the hyperchaotic behavior can be discriminated from a chaotic region by checking the full set of Lyapunov exponents. Second, more unanticipated regularities can be illustrated carefully by zooming in on a Lyapunov fractal image with a fine resolution, such as periodic and chaotic hub cascades, infinite-hierarchy nested spirals, and phase similarities and recurrences.[32] And finally, the artistic sensibilities and the aesthetic judgments, to some extent, have been replaced by precise mathematical formulas.

### 4.1. The 1D case

There are two bifurcation parameters, $a$ and $b$, in map (5). The $a$ and $b$ can be either identical or independent. If $a = b$, it is a familiar case that we have encountered when dealing with the logistic map. In this case, lots of periodic sequences of parameters, such as AB (Lyapunov fractal) and AABAB (Jellyfish) in dealing with the 1D quadratic maps, can be taken as the control sequence of parameters. Figures 8(a)–8(d) display the comprehensive details and gradually magnify the details of the sketches of the Lyapunov fractals with sequence AB. More surprisingly, as shown in Fig. 8(c), a chaotic hub is encircled by a periodic hub at the end of the infinite-hierarchy nested spirals, which can be observed in each rostrum of the shrimps. What is more, one of the most surprising findings is

that a bosmina (Figs. 8(a), 8(b), and 8(d)) manages to escape from two shrimps' siege (Figs. 8(a) and 8(b)). However, to avoid destroying the whole appearance, we do not superimpose any labels, e.g., boxes, arrows, or texts, on these figures to highlight what is coming. Clearly, the spinal curves, which denote the minimum Lyapunov exponents, can be observed in Fig. 8. If $a$ and $b$ are independent, we can concentrate only on the dynamics in the $a$–$b$ plane, which is omitted here due to space limitations.

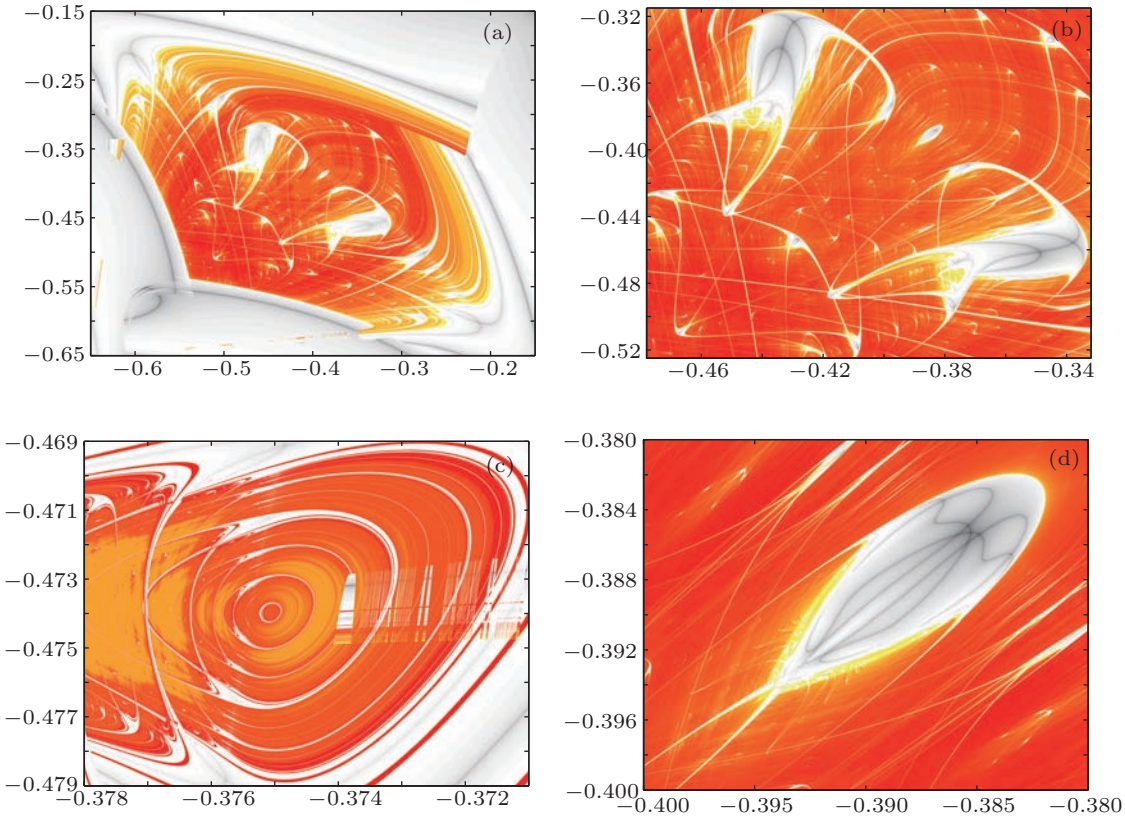



**Fig. 8.** (colour online) Lyapunov fractals of map (5) with identical parameters. Panel (a) shows a segment of the Lyapunov fractal. Panels (b)–(d) show fractals of shapes of two shrimps and one bosmina, infinite-hierarchy nested spirals, and one bosmina, respectively.

## 4.2. The 2D case

This case occurs when iterating map (1) from different start points with $x_0 \neq y_0$. In Fig. 9, the regions with both maximal and minimal Lyapunov exponents greater than 0, denoted as the hyperchaos, are discriminated from the chaotic regions, where only the maximal Lyapunov exponents greater than 0 are concerned originally. However, in this way, we will lose the information about the coexistence of multiple attractors in comparison with the study in the parameter space (see Fig. 3).

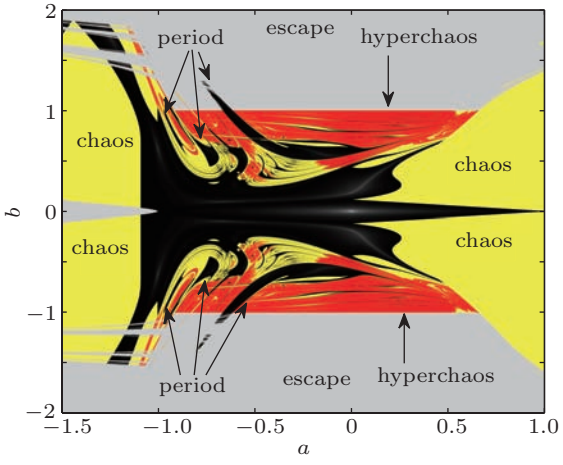



**Fig. 9.** (colour online) Lyapunov fractal of map (1).

## 5. Conclusion

In this paper, we report on numerical investigations about the relative abundance and the fractal structures of a nonlinear quadratic map. Due to the existence of exponential terms and endomorphism coupling, the map suffers fast convergence and divergence symmetrically in the parameter space. On the whole, the map and its derivatives present inherent and extraordinary structures, and some of them are unique.

## Acknowledgments

The first author thanks Dr. Leung C A from City University of Hong Kong for offering the Ph. D program foundation, and professor Leung Y A from City University of Hong Kong and Dr. Han X P from Shandong Normal University for their useful comments.

## References

[1] May R M 1976 *Nature* **261** 459
[2] Hénon M 1976 *Comm. Math. Phys.* **50** 69
[3] Mira C, Gardini L, Barugola J and Cathala J 1996 *Chaotic Dynamics in Two-dimensional Noninvertible Maps* (Singapore: World Scientific)
[4] Meng J D, Bao B C and Xu Q 2011 *Acta Phys. Sin.* **60** 010504 (in Chinese)
[5] Wang X Y and Luo C 2005 *Acta Mech. Sin.* **37** 346 (in Chinese)
[6] Qu S X, Lu Y Z, Zhang L and He D R 2008 *Chin. Phys.* B **17** 4418
[7] Wang X Y and Wang M J 2008 *Acta Phys. Sin.* **57** 731 (in Chinese)
[8] Sun F Y and Lü Z W 2011 *Chin. Phys.* B **20** 040506
[9] Wang X Y and Wang L L 2011 *Chin. Phys.* B **20** 050509
[10] Ott E 2002 *Chaos in Dynamical Systems* (Cambridge: Cambridge University Press)
[11] Jia H Y, Chen Z Q and Ye F 2011 *Acta Phys. Sin.* **60** 010203 (in Chinese)
[12] Li Q H and Tan J Y 2011 *Chin. Phys.* B **20** 040505
[13] Zhou G H, Bao B C, Xu J P and Jin Y Y 2010 *Chin. Phys.* B **19** 050509
[14] Rempe L 2007 *Anna. Acad. Sci. Fen. Math.* **32** 353
[15] Markus F and Dierk S 2008 *Ergod. Th. Dynam. Sys.* **0** 1
[16] Mira C 1987 *Chaotic Dynamics: From the One-dimensional Endomorphism to the Two-dimensional Diffeomorphism* (Singapore: World Scientific)
[17] Bao B C, Kang Z S, Xu J P and Hu W 2009 *Acta Phys. Sin.* **58** 1420 (in Chinese)
[18] Udwadia F E and Raju N 1998 *Physica* D **111** 16
[19] Li E Y, Li G Y, Wen G L and Wang H 2009 *Nonlin. Anal.* **70** 3227
[20] Ueta T, Tsuji S, Yoshinaga T and Kawakami H 2001 *ISCAS* **2** 755
[21] Ma J H and Chen Y S 2001 *Appl. Math. Mech.* **22** 1240 (in Chinese)
[22] Bonatto C and Gallas J A C 2008 *Phys. Rev. Lett.* **101** 054101
[23] Xu J, Long K P, Daniele F P and Taha A K 2010 *Chin. Phys. Lett.* **27** 020504
[24] Mo J, Li Y Y, Wei C L, Yang M H, Gu H G, Qu S X and Ren W 2010 *Chin. Phys.* B **19** 080513
[25] Wang X Y and Meng Q Y 2004 *Acta Phys. Sin.* **53** 388 (in Chinese)
[26] Gallas J A C 1993 *Phys. Rev. Lett.* **70** 2714
[27] Gallas J A C 2010 *Int. J. Bifur. Chaos* **20** 197
[28] Ramírez-Ávila G M and Gallas J A C 2010 *Phys. Lett.* A **375** 143
[29] Song Y Z, Zhao G Z and Qi D L 2006 *Chin. Phys.* **15** 2266
[30] Zou H L, Xu J X and Jiang J 2010 *Chin. Phys.* B **19** 059201
[31] Markus M and Hess B 1989 *Comp. Graph.* **13** 553
[32] Bonatto C, Gallas J A C and Ueda Y 2008 *Phys. Rev.* E **77** 026217